



# Shielding effectiveness performance of polyaniline-NiFe<sub>2</sub>O<sub>4</sub>:Cu composites for sub-8 GHz applications

Ethem İlhan Şahin<sup>1</sup> · Mehriban Emek<sup>2</sup> · Jamal Eldin F. M. Ibrahim<sup>3,4</sup> · Görkem Yumuşak<sup>5</sup> · Mesut Kartal<sup>6</sup>

Received: 31 January 2023 / Accepted: 21 March 2023  
© The Author(s) 2023

## Abstract

Herein, NiFe<sub>2</sub>O<sub>4</sub> doped Cu was synthesized using a mixed-oxide method to investigate its potential for creating composites with high microwave shielding effectiveness. The compound NiFe<sub>2-x</sub>Cu<sub>x</sub>O<sub>4</sub> was synthesized with x values of 0.1, 0.3 and 0.5, respectively. After sintering at 1250 °C for 4 h, single-phase Ni ferrite was formed. To analyze the phase composition and the structure of the synthesized compound, X-ray diffraction, scanning electron microscopy, and energy-dispersive X-ray spectroscopy were employed. The study's findings showed that NiFe<sub>2-x</sub>Cu<sub>x</sub>O<sub>4</sub> did not exhibit a second phase. To create composites with high microwave shielding effectiveness, polyaniline-NiFe<sub>2</sub>O<sub>4</sub>:Cu composites were fabricated using a hot-pressing technique, with compositions of NiFe<sub>1.9</sub>Cu<sub>0.1</sub>O<sub>3.95</sub>, NiFe<sub>1.7</sub>Cu<sub>0.3</sub>O<sub>3.85</sub> and NiFe<sub>1.5</sub>Cu<sub>0.5</sub>O<sub>3.75</sub> with the aniline. The weight ratios of Cu-added nickel ferrite and aniline were changed from 1:1 to 1:3, and epoxy resin was used. Using a two-port vector network analyzer, the polyaniline-NiFe<sub>2</sub>O<sub>4</sub>:Cu composites' microwave shielding effectiveness performance was examined in the range between 0 and 8 GHz. The study found that the shielding effect of the composites could be easily modified by changing the amount of polyaniline present in the specimens for the appropriate frequency bands. At 6.82 GHz, using a sample with a thickness of 2.0 mm, a minimum shielding effect performance of -29.74 dB was achieved. Overall, the results of this study demonstrate the potential of polyaniline-NiFe<sub>2</sub>O<sub>4</sub>:Cu composites as effective microwave shielding materials.

**Keywords** Microwave shielding effectiveness · NiFe<sub>2</sub>O<sub>4</sub> · Polymer-matrix composite · Polyaniline

✉ Jamal Eldin F. M. Ibrahim  
jamalfadoul@gmail.com

Extended author information available on the last page of the article

## 1 Introduction

Perovskite ceramic materials are attracting huge interest nowadays due to their fascinating properties, which lead to different optoelectronic applications (Tıhtih et al. 2021, 2023; Ibrahim et al. 2017, 2019; Lökçü 2013). One of these applications includes microwave shielding (Pratap et al. 2018, 2021; Peymanfar et al. 2020a, 2021a). Electromagnetic shielding can be defined as the process of reflecting electromagnetic wave's absorption and scattering, not entering or leaving a certain area. It is expressed as the sum of absorption and scattering. It mainly works with the Faraday Cage principle. The Faraday cage is based on the principle of inducing the effect of the wave in a direction to be transmitted by electron movements on a conductive surface. It also provides weakening of the part in the grounded state. It also shows the reflecting effect depending on the surface conductor density of the Faraday cage. The absorption effect is that the electromagnetic waves turn into heat by multiple scattering and absorption during the transition depending on the ambient dielectric and magnetic properties (Yuping et al. 2005; Peymanfar et al. 2021b). The shielding materials can be divided into two groups: (1) wave-reflection dominating materials and (2) wave-absorption dominating materials. Magnetic materials like spinel ferrites, nonconductor materials like carbon nanotubes, graphite and graphene, and conductive polymers are some of the most common wave absorber materials (Li et al. 2006; Rohini 2014; Pratap et al. 2020; Peymanfar et al. 2020b).

Shielding composites are typically designed in one of two forms: layered or embedded. Layered components are created by a stepwise coating of the shielding ingredients. One type of material that has been extensively studied for its potential as a shielding component is  $MFe_2O_4$  ( $M = Ni, Zn, Cu, Co, \text{etc.}$ ), which is a type of spinel ferrite. In these materials, every divalent transition metal ion is denoted by the letter M, and oxygen ions create face-centred cubic lattices within that arrangement. The metal ions are either surrounded by four (Tetrahedral) or six (Octahedral) oxygen ions. The properties of these materials are determined by the arrangement of cation tetrahedral (A) and octahedral (B) sites (metal ions). The distribution of cations in these structures is highly dependent on the preparation process, particle size, and dopants. Therefore, the magnetic, electrical, and optical properties of ferrites can be modified by the form and quantity of dopants. A variety of studies have been carried out in this direction to better understand the effects of dopants on the properties of ferrite materials (Ata-Allah et al. 2005; Birajdar et al. 2005; Peymanfar et al. 2021c).

$NiFe_2O_4$  spinel ferrite is a ferromagnetic composite with a large magnetic loss factor and strong electromagnetic (EM) incident attenuation. Dixit et al. (2012) investigated how Ce and Gd ions affected the magnetic characteristics of  $NiFe_2O_4$  nanoparticles using magnetic resonance spectroscopy. They concluded in contrast to Gd, Ce has a high magnetization. Doping with Ce is thus more appropriate from the standpoint of implementation.  $NiFe_2O_4$  ceramics are extensively used in magnetic and microwave devices, like electromagnetic shielding regions and microwave absorber materials. These are commonly researched owing to their strong electromagnetic strength, superior chemical permanence and mechanical toughness, strong coerciveness and medium saturation magnetization, making them a reasonable choice for use as tender magnets and short-loss materials at high frequencies

$NiFe_2O_4$  is a well-known microwave-absorbing material; however, its use is limited by disadvantages such as small dielectric loss and wide area density. To overcome this limitation, researchers have investigated mixing or blending Cu-doped ferrite powder with

non-magnetic polymers. One promising polymer is polyaniline (PANI), which not only has specified reflective loss but also has more absorption loss to achieve electromagnetic shielding. Thus, it can meet the high absorption and low reflection requirements needed for effective shielding. Additionally, the performance of microwave shielding effectiveness depends on the matching of the impedance of the surface of the material to the irradiation. PANI improves the matching impedance by enhancing the transmission between the ingredients of the composites. Therefore, the use of PANI in conjunction with Cu-doped ferrite powders has been shown to significantly improve the performance of microwave shielding composites, making them suitable for wideband absorption bandwidth applications. Therefore  $\text{NiFe}_2\text{O}_4$  can be utilized with the polymer matrix, such as polypyrrole (PPY) (Lee et al. 2002) and polyaniline (PANI) (Chen et al. 2013), to create an efficient EMI shielding material (Jaiswal et al. 2020). Due to its peculiar chemical and physical features, low cost, improved ecological stability, and ease of synthesis, polyaniline (PANI) is a useful conducting polymer (Yang et al. 2010; Ansari and Mohammad 2011). PANI, polymerized out of a low-cost aniline monomer, has drawn significant concern owing to its tunable electrical conductivity and environmental sustainability (Gu et al. 2013). In addition, conductive PANI has been deemed a suitable microwave absorption substance (MAM) for the control of dielectric loss. Because of its microwave absorber abilities, PANI was also used on textiles (Chen et al. 2013). Nevertheless, PANI still has some disadvantages, such as poor microwave absorber capacity and a narrow absorption band, which limits its potential uses. In efforts to resolve these issues and enhance its EMI efficiency, we recommend merging PANI with inorganic magnetic particles such as Ni ferrite ( $\text{NiFe}_2\text{O}_4$ ) (Chung 2000). It has been understood that composite materials are needed to provide better shielding rather than meeting the microwave SE requirements of a single material.

Research has shown that by packing  $\text{NiFe}_2\text{O}_4$  nanocrystals with composites to a thickness of 3.5 mm, a minimum reflective loss of  $-24$  dB at 9.5 GHz and a RL of  $-10$  dB at 8.5 to 13.0 GHz can be achieved (Ren et al. 2017). Additionally, a colemanite/PANI/ $\text{SiO}_2$  composite structure, manufactured at a thickness of 1.5 mm, provided the highest SE value of  $-41.1$  dB at 16.09 GHz (Şahin et al. 2020). In another study, polyaniline- $(\text{La}_2\text{Ti}_2\text{O}_7:\text{Er}, \text{Yb})$  composites demonstrated an SE (insertion loss) of  $-34.37$  dB at 6.27 GHz (Şahin et al. 2021). Furthermore, a Wollastonite/PANI/Colemanite composite was found to have a SE value of  $-41.65$  dB at 6.26 GHz and a thickness of 1.5 mm (Başaran 2020). Another literature study evaluated the EMP shielding protection of mortar mixed with SiC and graphite (Park and Cho 2022). In addition, the shielding efficiency of a frequency selective surface (FSS) was measured at MHz frequencies for the GSM system (Jangi Golezani et al. 2022). Besides, radiation SE of concrete containing oxidizing slag aggregate from electric arc furnaces was examined as another instance in the research (Lim et al. 2019).

In this investigation, Cu-doped Nickel ferrites along the compositions of  $\text{NiFe}_{1.9}\text{Cu}_{0.1}\text{O}_{3.95}$ ,  $\text{NiFe}_{1.7}\text{Cu}_{0.3}\text{O}_{3.85}$  and  $\text{NiFe}_{1.5}\text{Cu}_{0.5}\text{O}_{3.75}$  were synthesized utilizing the mixed-oxide approach. EMI shielding characteristics of new PANI- $\text{NiFe}_2\text{O}_4$ :Cu composites were investigated using the best possible parameters for the first time. The phases of specimens were determined by X-ray diffractometry (Bruker AXS-XRD-D2 Phaser) in order to determine the solubility limit of each additive and the secondary phases formed in Cu-doped sintered pellets. The microstructural and topographical features of the fracture surfaces of the specimens were investigated using SEM (Jeol JSM 5910 LV) was used for Şahin (2022); the magnetic hysteresis results were measured by VSM (Cryogenic Limited PPMS). The microwave SE properties of the PANI- $\text{NiFe}_2\text{O}_4$ :Cu with epoxy composite materials were tested at 0–8 GHz, including certain radar frequencies, using (R&S FSH-K42) two-port vector network analyzer device.

The  $\text{NiFe}_2\text{O}_4$  (PDF Card No: 44-1485) compound is considered a suitable host for Cu atom. The Cu ( $x=0.1, 0.3$  and  $0.5$ ) element is doped into  $\text{NiFe}_{2-x}\text{Cu}_x\text{O}_4$  composition to replace Fe ion since they have very close ionic radii. Upon the doping process, the solubility was raised (within the solubility limit) and designed its environment with respect to Cu element, increased the wave interference by the rising surface area and enhanced the effectiveness of shielding (Şahin 2019).

## 2 Experimental

### 2.1 Cu-added nickel ferrite preparation

Using a mixed-oxide process, Cu-doped  $\text{NiFe}_2\text{O}_4$  powder was generated. Powders of NiO (Sigma-Aldrich, 99.9%),  $\text{Fe}_2\text{O}_3$  (Sigma-Aldrich: 96.5%), and CuO (Alfa Aesar: 99.99%) were blended in stoichiometric proportions according to  $\text{NiFe}_{2-x}\text{Cu}_x\text{O}_4$  compositions in an ethanol medium in a plastic bottle for 20 h, where  $x=0.1, 0.3, 0.5$ , respectively. The slurries were first left to dry for 24 h at  $100\text{ }^\circ\text{C}$ , and then they would be calcinated for 4 h at  $600\text{ }^\circ\text{C}$  in an airtight crucible composed of Al to minimize evaporation losses, which were measured by weighing the specimens before and after calcination. The calcinated powders were crushed in an agate mortar before being pressed into specimens with a diameter of 10 mm and a thickness of 1–2 mm using uni-axial pressing with a pressure of 2 MPa. After burying the pellets in  $\text{NiFe}_2\text{O}_4$  powder, they were sintered for 4 h at a temperature range between 1200 and  $1400\text{ }^\circ\text{C}$  with a cooling and heating rate of  $250\text{ }^\circ\text{C}/\text{h}$  to reduce volatile species loss. The single-phase  $\text{NiFe}_2\text{O}_4$  were heat treated at  $1200\text{--}1300\text{ }^\circ\text{C}$ , while Cu-added  $\text{NiFe}_2\text{O}_4$  reactants powders were heat treated at  $1250\text{ }^\circ\text{C}$  after being calcinated at  $600\text{ }^\circ\text{C}$ . X-ray diffractometry with Cu-K $\alpha$  radiance ( $\lambda=1.5406\text{ \AA}$ ) in the range of  $2\theta:10\text{--}70^\circ$  at a scanning speed of  $1^\circ/\text{min}$  was used to describe the phases in the doped heat-treated specimens. X-ray powder diffractometry was used to determine the solubilities limit, which is defined as the maximum quantity of doping that can be done without affecting the primary structure ( $\text{NiFe}_2\text{O}_4$ ). The samples were covered with Au/Pd alloy using a sputter coater before being analyzed for fracture surfaces with SEM (JEOL 5910LV) at 20 kV. A dispersive spectrometer (EDS, Oxford-Inca-7274) was used for the chemical analysis, while SEM was employed to determine the topographical feature and examine the microstructure. The microwave shielding effects of the PANI- $\text{NiFe}_2\text{O}_4$ :Cu composite materials were measured between 0 and 8 GHz using the 2-port VNA (R & S FSH-K42) instrument.

### 2.2 Producing of polyaniline/ $\text{NiFe}_2\text{O}_4$ :Cu composites

The Nickel ferrite samples, which have the compositions of  $\text{NiFe}_{1.9}\text{Cu}_{0.1}\text{O}_{3.95}$ ,  $\text{NiFe}_{1.7}\text{Cu}_{0.3}\text{O}_{3.85}$  and  $\text{NiFe}_{1.5}\text{Cu}_{0.5}\text{O}_{3.75}$  (accounted for 100 wt% and 33 wt% of aniline quantities, respectively), and 1 ml aniline monomer were added to a solution of 35 ml hydrochloric acid ( $0.1\text{ mol L}^{-1}$ ) and mechanically mixed for 30 min. In a 15 ml hydrochloric acid solution, 2.49 g of ammonium persulfate (APS) was dissolved. Drop by drop, with vigorous stirring, the APS solution was then added to the previously prepared solution. In an ice-water bath, polymerization was completed at  $0\text{ }^\circ\text{C}$  for 12 h. The composites were made by sifting the resulting mixture, washing it with deionized water and ethanol, and then vacuum-drying it for 24 h at  $60\text{ }^\circ\text{C}$ . The influence of the polyaniline ingredient on the effectiveness of EM shielding was investigated using PANI/  $\text{NiFe}_2\text{O}_4$  composites

with varied molar ratios (Aniline/NiFe<sub>1.9</sub>Cu<sub>0.1</sub>O<sub>3.95</sub>, Aniline/NiFe<sub>1.7</sub>Cu<sub>0.3</sub>O<sub>3.85</sub>, and Aniline/NiFe<sub>1.5</sub>Cu<sub>0.5</sub>O<sub>3.75</sub>) = (3:1, 1:1). The Cu-added NiFe<sub>2</sub>O<sub>4</sub> with a PANI base were produced as new composite. PANI-NiFe<sub>2</sub>O<sub>4</sub>:Cu was created in various ratios with hot pressing.

## 2.3 Preparation of epoxy-polyaniline/NiFe<sub>2</sub>O<sub>4</sub>:Cu composites

PANI/Cu added Ni ferrite composition powders and epoxy were molded and cured to create the composites. The prepared powders were mixed with epoxy in a 2:1 weight ratio. The molding was completed in a 5 MPa hydraulic press at 100 °C for 1 h. The powders were pressed into 20 mm diameter and 2 mm thick pellets for shielding effectiveness tests. Varying concentrations of aniline/Cu-added Ni ferrite, such as 1/1 and 3/1, were used to create SE composites.

## 2.4 Characterization techniques

The composites under investigation were thoroughly characterized using various analytical techniques. X-ray diffraction (XRD) analysis was performed using a Bruker/Alpha-T instrument to determine the phases present in the samples. To investigate the microstructure and morphology of composites, scanning electron microscopy (SEM) was carried out using a JEOL 5910 LV instrument. To improve the conductivity of the powder samples, they were placed on carbide tape and coated with an Au/Pd alloy. The chemical composition was determined using dispersive spectrometry (EDS) with an Oxford-Inca-7274 instrument. The microwave shielding effectiveness of the Cu-doped NiFe<sub>2</sub>O<sub>4</sub>:PANI composites, with a thickness of 2 mm, was measured over the frequency range of 0–8 GHz, including some radar frequency bands, using a two-port vector network analyzer (R&S FSH8-R&S FSH-K42) device. The magnetic properties of the CuO-doped NiFe<sub>2</sub>O<sub>4</sub> samples, sintered at 1250 °C, were studied at room temperature (25 °C) using magnetic hysteresis measurements (VSM) with a Cryogenic Limited PPMS brand device. With the VSM measurement, the magnetic properties of the Cu-doped and polyaniline-based nickel ferrite powder samples were characterized in a certain magnetic field range at room temperature. These comprehensive analyses provide a better understanding of the structure, composition, and magnetic properties of the Cu-doped NiFe<sub>2</sub>O<sub>4</sub>:PANI composites.

# 3 Results and discussion

## 3.1 XRD investigations of Cu-doped nickel ferrite

The addition of Cu ions into the NiFe<sub>2</sub>O<sub>4</sub> (PDF Card No: 003-0875) compound to replace Fe ions was carried out due to the similarity in their ionic radii values. This process involved the synthesis of NiFe<sub>2-x</sub>Cu<sub>x</sub>O<sub>4</sub> compositions, where x varied between 0.1 and 0.6. To obtain single-phase structures, specimens with x values of 0.1, 0.3, and 0.5 were heat-treated for four hours at 1250 °C using mixed oxide methods. The resulting powders exhibited excellent homogeneity, which facilitated diffusion during the heating phase and eliminated any possible intermediary phases. XRD analysis (Fig. 1) revealed no secondary phases in the powders, except for the 0.6 mol% Cu-added pattern, which showed the emergence of the CuO (PDF Card No: 44-706) secondary phase. These findings suggest that the solubility limit of Cu in nickel ferrite ranges from x = 0.5 to x = 0.6. Table 1 shows

**Fig. 1** X-ray diffraction patterns of Cu-doped  $\text{NiFe}_{2-x}\text{Cu}_x\text{O}_4$  compound with (Cu,  $x = 0.1, 0.3, 0.5, 0.6$ ) sintered for 4 h at  $1250^\circ\text{C}$

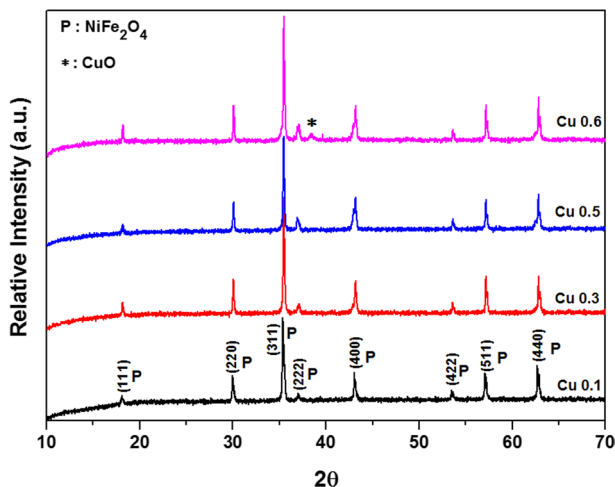


**Table 1** Lattice constant of the prepared samples

Sample	Lattice constant ( $\text{\AA}$ )
$\text{NiFe}_2\text{O}_4$	8.336
Cu 0.1 doped $\text{NiFe}_2\text{O}_4$	8.3434
Cu 0.3 doped $\text{NiFe}_2\text{O}_4$	8.3552
Cu 0.5 doped $\text{NiFe}_2\text{O}_4$	8.3559
Cu 0.6 doped $\text{NiFe}_2\text{O}_4$	8.3568

the XRD structural parameters of the produced sample, indicating that the synthesis of  $\text{NiFe}_2\text{O}_4$  is highly temperature-dependent, and single-phase  $\text{NiFe}_2\text{O}_4$  production requires high temperatures. The addition of Cu ions had a significant impact on the formation temperatures of the  $\text{NiFe}_2\text{O}_4$  single-phase.

### 3.2 SEM analysis of Cu-doped nickel ferrite

The SEM images of the Cu-added Nickel ferrite structure showed that for  $x=0.1$ , there was only one phase present (Fig. 2a), but as the  $x$  value was increased to 0.6, a secondary phase emerged (Fig. 2b). The secondary phase was identified as CuO, while the single phase was determined to be Cu-containing Ni ferrite. The EDS study results, depicted in Fig. 2c, d, indicated that the Cu-doped  $\text{NiFe}_2\text{O}_4$  particles had a composition (% 24.08 Ni, % 48.39 Fe, % 26.16 O, % 1.37 Cu) that was in line with the predicted composition. As the concentration of Cu increased, the amount of the secondary phase also increased (Fig. 2b), and the ratio of Cu in the structure grew, as per the EDS analysis performed on the secondary phase. Moreover, it is apparent that different Cu-doped ratios have a significant impact on the particle sizes of Cu-doped  $\text{NiFe}_2\text{O}_4$  when viewed from the standpoint of grain size. Interestingly, the secondary phase development observed in the EDS images was in good agreement with the XRD data, suggesting that both techniques complement each other in characterizing the structure and composition of Cu-doped  $\text{NiFe}_2\text{O}_4$ . These findings provide valuable insights into the structural and compositional changes that occur

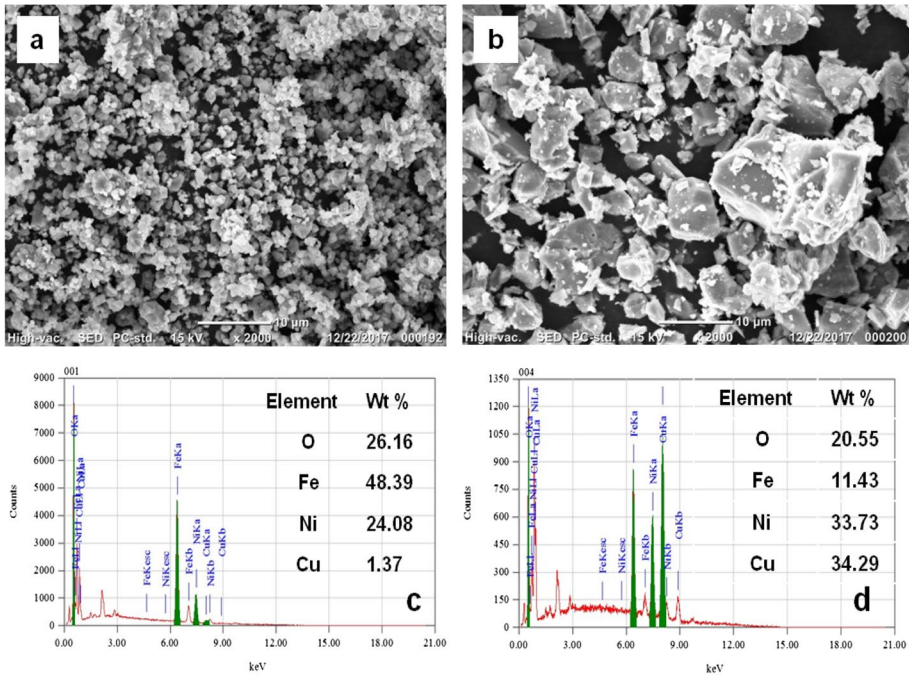


**Fig. 2** SEM pictures of a Cu-added NiFe<sub>2</sub>O<sub>4</sub> composition that was sintered for 4 h at 1250 °C. **a** x = 0.1 at × 2,000, **b** x = 0.6 at × 2,000, **c** EDS investigation of Cu-doped NiFe<sub>2-x</sub>Cu<sub>x</sub>O<sub>4</sub> for x = 0.1 **d** EDS analysis of Cu-doped NiFe<sub>2-x</sub>Cu<sub>x</sub>O<sub>4</sub>, secondary phase CuO for x = 0.6

in Cu-doped NiFe<sub>2</sub>O<sub>4</sub> and can aid in the optimization of this material for various technological applications.

### 3.3 Magnetic properties of NiFe<sub>2</sub>O<sub>4</sub>:Cu composites and PANI/NiFe<sub>2</sub>O<sub>4</sub>:Cu composites

To examine the impact of dopants on the magnetic characteristics, magnetic measurements of CuO-doped NiFe<sub>2</sub>O<sub>4</sub> patterns heat treated at 1250 °C were carried out at room temperature (25 °C). In Fig. 3a, CuO-doped NiFe<sub>2</sub>O<sub>4</sub> patterns' magnetization is displayed as a function of the magnetic field (M–H). The measured magnetic parameter values of the produced samples are shown in Table 2. With a saturation magnetization (M<sub>s</sub>) of roughly 41.8 emu/g, the 0.1% CuO (x = 0.1) doped NiFe<sub>2-x</sub>Cu<sub>x</sub>O<sub>4</sub> sample demonstrated optimal ferromagnetic behaviour. When the concentration of the Cu doping element rose to x = 0.3, the saturation magnetization increased slightly, reaching almost 43.2 emu/g. When the concentration of Cu element rose to x = 0.5, M<sub>s</sub> value decreased to 36.5. It is understood that with the increase of the additive amount of Cu element, the M<sub>s</sub> also increases and decreases back as x = 0.5. Neel's molecular field theory can account for the magnetization of spinel ferrite. This theory demonstrates that the exchange between A–B sites has a stronger interaction than the exchange between A–A and B–B sites.

Due to the occupancy of CuO on B-sites when x = 0.1, the concentration of Fe<sup>+3</sup> ions at octahedral B-sites falls. Therefore, the reduction in saturation magnetization is

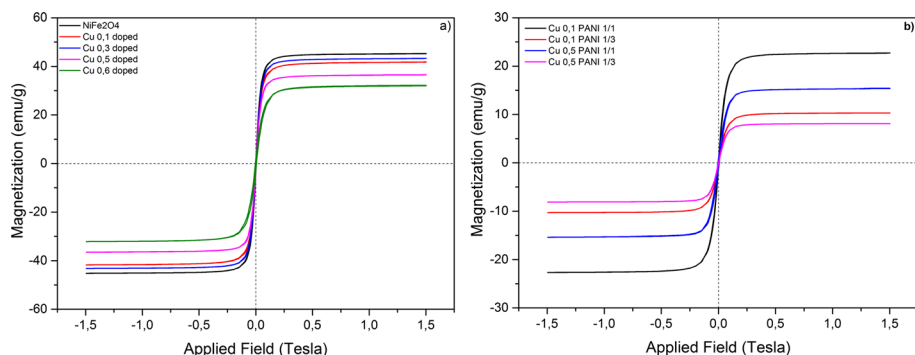


**Fig. 3** **a** Magnetic hysteresis loops for Cu-added NiFe<sub>2</sub>O<sub>4</sub> ( $x = 0.1, 0.2, 0.3, 0.5$ ) heat treated at 1250 °C for 4 h. **b** Magnetic hysteresis loops for Cu-doped NiFe<sub>2</sub>O<sub>4</sub> ( $x = 0.1, 0.5$ ) using polyaniline (1/3, 1/1) heat treated at 1250 °C for 4 h

**Table 2** VSM (measured magnetic parameters) of various compositions for synthesized samples

Sample	VSM (emu/g)	Sample	VSM (emu/g)
Cu 0.1 doped NiFe <sub>2</sub> O <sub>4</sub>	41.8	Cu 0.1 doped NiFe <sub>2</sub> O <sub>4</sub> PANI 1/1	22.7
Cu 0.3 doped NiFe <sub>2</sub> O <sub>4</sub>	43.2	Cu 0.1 doped NiFe <sub>2</sub> O <sub>4</sub> PANI 1/3	10.3
Cu 0.5 doped NiFe <sub>2</sub> O <sub>4</sub>	36.5	Cu 0.5 doped NiFe <sub>2</sub> O <sub>4</sub> PANI 1/1	15.4
Cu 0.6 doped NiFe <sub>2</sub> O <sub>4</sub>	32	Cu 0.5 doped NiFe <sub>2</sub> O <sub>4</sub> PANI 1/3	8.12

caused by the alteration in the magnetic structure. The dispersion of nonmagnetic CuO ions in sites A and B may be responsible for the reduction of  $x \geq 0.5$ . A minor drop down to 32 emu/g was seen in Ms when the NiFe<sub>2-x</sub>Cu<sub>x</sub>O<sub>4</sub> specimen was added with  $x = 0.6$  CuO.

As the Polyaniline concentration decreased from 1:1 to 1:3, the saturation magnetization of the samples decreased, as illustrated in Fig. 3b. In addition, the magnetic hysteresis loops for CuO-doped NiFe<sub>2-x</sub>Cu<sub>x</sub>O<sub>4</sub> specimens ( $x = 0.1$ ) with varying Polyaniline concentrations (1/3 and 1/1) were found to be dependent on the magnetic field at 1250 °C. Both specimens exhibited different ferromagnetic behaviours. The sample with a PANI content of 1/3 showed a smaller Ms value of approximately 10.3 emu/g, whereas the sample with a PANI content of 1/1 showed a higher Ms value of about 22.7 emu/g. Similarly, the CuO-doped NiFe<sub>2-x</sub>Cu<sub>x</sub>O<sub>4</sub> specimens ( $x = 0.5$ ) with different Polyaniline contents (1/3 and 1/1) exhibited comparable ferromagnetic activity, with Ms values of 8.12 and 15.4 emu/g, respectively. These findings suggest that Polyaniline content has a significant influence on the magnetic properties of CuO-doped NiFe<sub>2-x</sub>Cu<sub>x</sub>O<sub>4</sub>.

### 3.4 Measurements of Cu-added nickel ferrite's EMI shielding effect

The results of a study on the electromagnetic shielding effectiveness of various composites are presented in Fig. 4 and Table 3. The purpose of the SE test is to determine how much of the incoming EM wave passes through the composite material (Keykavous-Amand and Peymanfar 2021). The results show that the epoxy-(PANI/NiFe<sub>2</sub>O<sub>4</sub>:Cu) composites had different SE characteristics depending on their composition. The epoxy-NiFe<sub>2</sub>O<sub>4</sub>:Cu

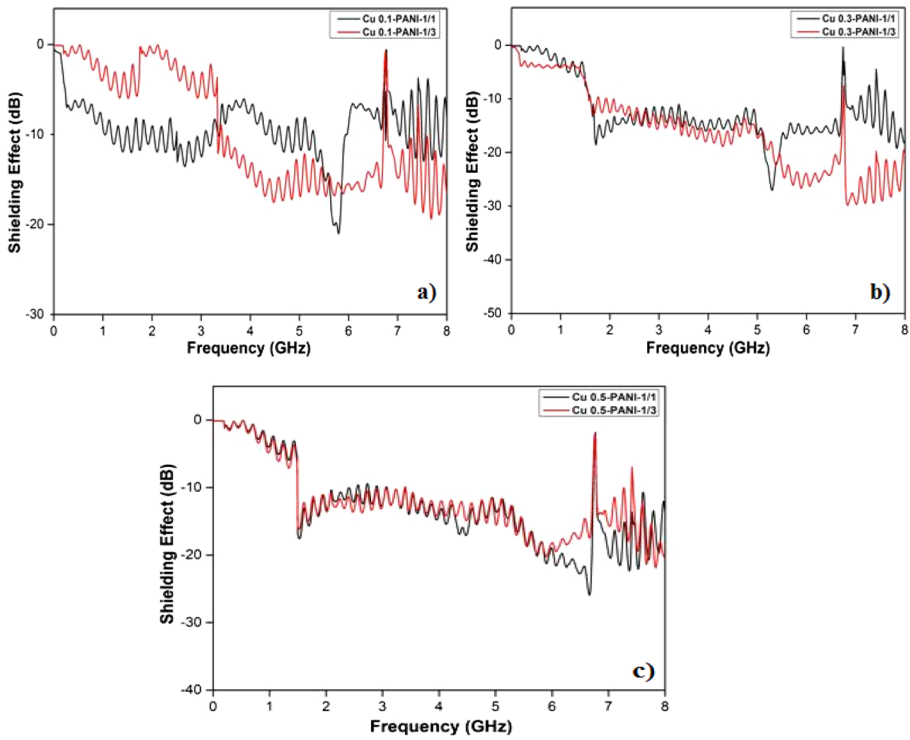


**Fig. 4** Microwave shielding features of the epoxy-(polyaniline/ $\text{NiFe}_{2-x}\text{Cu}_x\text{O}_4$ ) composites **a**  $x = 0.1$ , Ni ferrite/Aniline compositions of  $\text{NiFe}_{1.9}\text{Cu}_{0.1}\text{O}_{3.95}$  weight ratio was altered as 1/1, 1/3 **b**  $x = 0.3$ , Ni ferrite/Aniline compositions of  $\text{NiFe}_{1.7}\text{Cu}_{0.3}\text{O}_{3.85}$  weight ratio was altered as 1/1, 1/3 **c**  $x = 0.5$ , Ni ferrite/Aniline compositions of  $\text{NiFe}_{1.5}\text{Cu}_{0.5}\text{O}_{3.75}$  weight ratio was altered as 1/1, 1/3

**Table 3** The microwave absorption properties of synthesized powders compared with other results in the literature

Sample	SE	Frequency GHz	References
PANI/Cu-added $\text{NiFe}_2\text{O}_4$	-29.74 dB	6.82	This work
PANI/ $\text{BaFe}_{12}\text{O}_{19}$	-12.5 dB	7.8	Yang et al. (2010)
PANI/ $\text{MnFe}_2\text{O}_4$	-15.3 dB	10.4	Thirumalairajan et al. (2013)
PANI/ZnO	-41 dB	14.1	ur Rehman et al. (2019)
$\text{NiFe}_2\text{O}_4$ -graphene oxide	-46.8 dB	6.8	Zhao et al. (2016a)
$\text{NiFe}_2\text{O}_4$ nanosheets	-47.1	7.67	Zhao et al. (2016b)

composites/Aniline: 1/3 had a more pronounced impact on shielding effect characteristics than epoxy- $\text{NiFe}_2\text{O}_4$ :Cu composites/Aniline: 1/1.

Among the tested composites, the epoxy-PANI/Cu-added Ni ferrite composites ( $\text{NiFe}_{1.7}\text{Cu}_{0.3}\text{O}_{3.85}$ /Aniline: 1/3) demonstrated the highest overall SE performance with a maximum SE value of -29.74 dB at 6.82 GHz. This composition had a shielding effectiveness of less than -20 dB in the frequency ranges between 5.32 to 6.69 GHz and 6.79 to 7.4 GHz, and less than -10 dB in the frequency regions between 2.11 to 6.73 GHz and

6.77 to 8 GHz. The PANI/Ni ferrite composition ( $\text{NiFe}_{1.9}\text{Cu}_{0.1}\text{O}_{3.95}$  /Aniline: 1/1) had only one band with  $-21.04$  dB at 5.81 GHz, and its SE was less than  $-10$  dB in the frequencies bands between 2.52 to 3.06 GHz and 5.3 to 5.96 GHz. The SE of the composites is found to be highly dependent on their composition, and the epoxy-PANI/Cu-added Ni ferrite composites ( $\text{NiFe}_{1.7}\text{Cu}_{0.3}\text{O}_{3.85}$  /Aniline: 1/3) showed the best performance in terms of shielding effectiveness.

The frequency dependence of the shielding effectiveness (SE) of PANI/Cu-added Ni ferrite composites ( $\text{NiFe}_{1.5}\text{Cu}_{0.5}\text{O}_{3.75}$  /Aniline: 1/1) powders and epoxy is shown in Fig. 4c. The composite displayed only two SE bands, one at  $-26.02$  dB and another at  $-17.55$  dB, at 6.67 GHz and 1.53 GHz, respectively. The SE of this composite was less than  $-10$  dB in the frequency range of 1.48 GHz to 2.54 GHz, 3.08 GHz to 6.72 GHz, and 6.8 GHz to 8 GHz. The PANI/Cu-added Ni ferrite composite with the highest SE value was  $\text{NiFe}_{1.5}\text{Cu}_{0.5}\text{O}_{3.75}$  /Aniline: 1/3, with an SE of  $-21.89$  dB at 7.84 GHz, and it showed shielding effectiveness of less than  $-10$  dB in the frequency ranges between 1.48 to 3.37 GHz, 3.41 to 6.72 GHz, 6.79 to 7.4 GHz, and 7.44 to 8 GHz. The surface interactions, morphology and doping proportion, are key elements in adjusting polarizations, charge transformations and conductive loss (Peymanfar et al. 2020c, d). The interfacial polarization between polyaniline and single-phase Cu-doped  $\text{NiFe}_2\text{O}_4$  is critical for the electromagnetic shielding material, as the coherence (matching) of the impedance of the irradiation on the composite's surface impacts the SE performance.

The use of polyaniline in the composite material improves the matching impedance of the transmissions between the composite components. The interfacial polarization between polyaniline and Cu-added  $\text{NiFe}_2\text{O}_4$  greatly benefits the electromagnetic shielding composite material. As the crystallite size of  $\text{NiFe}_2\text{O}_4$  decreases, surface spin collisions increase, leading to a rise in the observed particle size distribution in the crystal structure and a corresponding increase in the shielding effect peak widths. The abrupt SE peaks arise due to the resonance effect of holder geometry and reflection (Peymanfar et al. 2020e). To minimize the eddy currents created by electromagnetic waves, conductive polymer polyaniline was utilized, as the permeability of higher-frequency materials can reduce the impact of eddy currents. PANI also results in electrical losses, making it suitable for mixing with  $\text{NiFe}_2\text{O}_4$  to adjust the dielectric shielding impact of the nickel ferrite and improve the effectiveness of the electromagnetic shielding. These results could have important implications for the development of new composite materials with improved electromagnetic shielding properties for use in various applications as it is comparable to the results in the literature (Table 4).

## 4 Conclusions

This research studied the potential use of composites made from polyaniline (PANI) and copper-doped nickel ferrite ( $\text{NiFe}_2\text{O}_4$ ) for microwave shielding effectiveness for the first time as far as it concerned. The following are the key findings:

1. PANI/Cu-added nickel ferrite composites have the potential to be used as effective microwave shielding materials due to their simple and low-cost manufacturing processes.
2. Cu doping into  $\text{NiFe}_{2-x}\text{Cu}_x\text{O}_4$ , even at high concentrations ( $x=0.5$ ), does not create a second phase and entirely dissolves, forming a single phase, as proven by XRD.

**Table 4** Shielding effectiveness of the epoxy-(polyaniline/NiFe<sub>2-x</sub>Cu<sub>x</sub>O<sub>4</sub>) composites with the ranges of shielding features in GHz

Sample	SE dB	Frequency GHz
NiFe <sub>1,9</sub> Cu <sub>0,1</sub> O <sub>3,95</sub> /Aniline: 1/1	-21.05	5.8
	-20	5.76–5.82
	-10	2.53–2.9, 5.32–5.91
NiFe <sub>1,9</sub> Cu <sub>0,1</sub> O <sub>3,95</sub> /Aniline: 1/3	-19.44	7.67
	-10	3.43–6.71, 6.79–7.39
NiFe <sub>1,7</sub> Cu <sub>0,3</sub> O <sub>3,85</sub> /Aniline: 1/1	-27.14	5.29
	-20	5.14–5.46
	-10	1.62–6.72, 7.63–8
NiFe <sub>1,7</sub> Cu <sub>0,3</sub> O <sub>3,85</sub> /Aniline: 1/3	-29.74	6.82
	-20	5.32–6.69, 6.79–7.4
	-10	2.11–6.73, 6.77–8
NiFe <sub>1,5</sub> Cu <sub>0,5</sub> O <sub>3,75</sub> /Aniline: 1/1	-26.02	6.67
	-17.55	1.53
	-10	1.48 to 2.54, 3.08 to 6.72, 6.8 to 8
NiFe <sub>1,5</sub> Cu <sub>0,5</sub> O <sub>3,75</sub> /Aniline: 1/3	-21.89	7.84
	-10	1.48 to 3.37, 3.41 to 6.72, 6.79 to 7.4, 7.44 to 8

- As PANI concentration increased, the lowest shielding effectiveness point for epoxy-PANI/NiFe<sub>2</sub>O<sub>4</sub>:Cu compositions changed toward higher frequencies.
- The NiFe<sub>1,7</sub>Cu<sub>0,3</sub>O<sub>3,85</sub>/Aniline: 1/3 composite achieved microwave shielding effectiveness at 6.82 GHz and 2.0 mm in thickness, with the lowest SE of -29.74 dB.
- The microwave shielding effectiveness of NiFe<sub>2</sub>O<sub>4</sub> with added copper varies greatly at high doping concentrations. However, the most effective shielding range is found in NiFe<sub>1,7</sub>Cu<sub>0,3</sub>O<sub>3,85</sub>/Aniline: 1/3 compositions, which have a shielding effectiveness of under -20 dB at frequencies between 5.32 to 6.69 GHz, and 6.79 to 7.4 GHz.
- The microwave shielding effectiveness of PANI-single phase Cu-doped NiFe<sub>2</sub>O<sub>4</sub> with various dopants might be examined in the radar and higher frequency bands for absorbance and shielding effect. These composites can be investigated as a guide in the development of armour and shielding materials in other frequency bands.

**Acknowledgements** This work has been edited in memorial of Salim Sahin and Emsal Sahin, Prof. Dr. Ayhan Mergen. This work is supported by Adana Alparslan Türkeş Science and Technology University.

**Authors' contributions** EİŞ, ME, JEFMI and MK wrote the main manuscript text and JEFMI, MK, prepared the formal analysis. MK did review & editing. EİŞ, ME and MK carried out the investigation of the microwave shielding effect and their interpretation. All authors reviewed the manuscript.

**Funding** Open access funding provided by University of Miskolc. The authors have not disclosed any funding.

**Data availability** All data generated or analyzed during this study are included in this article.

## Declarations

**Conflict of interests** Authors have no conflict of interest.

**Ethical approval** This declaration is “not applicable”.

**Open Access** This article is licensed under a Creative Commons Attribution 4.0 International License, which permits use, sharing, adaptation, distribution and reproduction in any medium or format, as long as you give appropriate credit to the original author(s) and the source, provide a link to the Creative Commons licence, and indicate if changes were made. The images or other third party material in this article are included in the article's Creative Commons licence, unless indicated otherwise in a credit line to the material. If material is not included in the article's Creative Commons licence and your intended use is not permitted by statutory regulation or exceeds the permitted use, you will need to obtain permission directly from the copyright holder. To view a copy of this licence, visit <http://creativecommons.org/licenses/by/4.0/>.

## References

- Ansari, M.O., Mohammad, F.: Thermal stability, electrical conductivity and ammonia sensing studies on p-toluenesulfonic acid doped polyaniline:titanium dioxide (pTSA/Pani:TiO<sub>2</sub>) nanocomposites. *Sens. Actuat. B Chem.* **157**(1), 122–129 (2011). <https://doi.org/10.1016/j.snb.2011.03.036>
- Ata-Allah, S.S., Fayek, M.K., Sayed, H.A., Yehia, M.: Effect of Zn doping on temperature and frequency dependence of dielectric permittivity and dielectric relaxation for synthesized tetragonal copper-gallium ferrite. *Mater. Chem. Phys.* **92**(1), 278–285 (2005). <https://doi.org/10.1016/j.matchemphys.2005.01.024>
- Başaran, S.: Manyetik dışı sisteminin sonlu elemanlar yöntemi ile analizi. *Eur. J. Sci. Technol.* **21**, 83–89 (2020). <https://doi.org/10.31590/ejosat.820561>
- Birajdar, D.S., Mane, D.R., More, S.S., Kawade, V.B., Jadhav, K.M.: Structural and magnetic properties of ZnxCu<sub>1.4-x</sub>Mn<sub>0.4</sub>Fe<sub>2</sub>O<sub>4</sub> ferrites. *Mater. Lett.* **59**(24–25), 2981–2985 (2005). <https://doi.org/10.1016/j.matlet.2005.03.072>
- Chen, D., Miao, Y.E., Liu, T.: Electrically conductive polyaniline/polyimide nanofiber membranes prepared via a combination of electrospinning and subsequent in situ polymerization growth. *ACS Appl. Mater. Interfaces* **5**(4), 1206–1212 (2013). <https://doi.org/10.1021/am303292y>
- Chung, D.D.L.: Materials for electromagnetic interference shielding. *J. Mater. Eng. Perform.* **9**(3), 350–354 (2000). <https://doi.org/10.1361/105994900770346042>
- Dixit, G., Singh, J.P., Srivastava, R.C., Agrawal, H.M.: Magnetic resonance study of Ce and Gd doped NiFe<sub>2</sub>O<sub>4</sub> nanoparticles. *J. Magn. Magn. Mater.* **324**(4), 479–483 (2012). <https://doi.org/10.1016/j.jmmm.2011.08.027>
- Fan, H.M., Yi, J.B., Yang, Y., Kho, K.W., Tan, H.R., Shen, Z.X., Feng, Y.P.: Single-crystalline MFe<sub>2</sub>O<sub>4</sub> nanotubes/nanorings synthesized by thermal transformation process for biological applications. *ACS Nano* **3**(9), 2798–2808 (2009)
- Gu, H., et al.: Epoxy resin nanosuspensions and reinforced nanocomposites from polyaniline stabilized multi-walled carbon nanotubes. *J. Mater. Chem. C* **1**(4), 729–743 (2013). <https://doi.org/10.1039/c2tc00379a>
- Ibrahim, J.-E., Ayhan Mergen, E., Şahin, İ., Basheer, H.: The effect of europium doping on the structural and magnetic properties of GdMnO<sub>3</sub> multiferroic ceramics. *Adv. Ceram. Prog.* **3**(4), 1–5 (2017)
- Ibrahim, J.F.M., Mergen, A., Parlak, U., Kurovics, E.: The influence of Cr doping on the structural and magnetic properties of HoMnO<sub>3</sub> multiferroic ceramics. In: *IOP Conference Series: Materials Science and Engineering*, vol. 613, No. 1, p. 012009–012016. IOP Publishing. <https://doi.org/10.1088/1757-899X/613/1/012009> (2019)
- Jaiswal, R., Agarwal, K., Pratap, V., Soni, A., Kumar, S., Mukhopadhyay, K., Prasad, N.E.: Microwave-assisted preparation of magnetic ternary core-shell nanofiller (CoFe<sub>2</sub>O<sub>4</sub>/rGO/SiO<sub>2</sub>) and their epoxy nanocomposite for microwave absorption properties. *Mater. Eng. B* **262**, 114711–114720 (2020). <https://doi.org/10.1016/j.mseb.2020.114711>
- Jangi Golezani, J., Kartal, M., Döken, B., Paker, S.: Triple-band frequency selective surface design effective over oblique incidence angles for GSM system. *IETE Res.* **68**(2), 1406–1410 (2022). <https://doi.org/10.1080/03772063.2019.1649210>
- Keykavous-Amand, S., Peymanfar, R.: Fabrication of clay soil/CuFe<sub>2</sub>O<sub>4</sub> nanocomposite toward improving energy and shielding efficiency of buildings. *Sci. Rep.* **11**(1), 1–13 (2021). <https://doi.org/10.1038/s41598-021-00347-x>
- Lee, C.Y., et al.: Electromagnetic interference shielding by using conductive polypyrrole and metal compound coated on fabrics. *Polym. Adv. Technol.* **13**(8), 577–583 (2002). <https://doi.org/10.1002/pat.227>

- Li, N., et al.: Electromagnetic interference (EMI) shielding of single-walled carbon nanotube epoxy composites. *Nano Lett.* **6**(6), 1–5 (2006)
- Lim, H.S., Lee, H.S., Kwon, S.J.: Mechanical properties and radiation shielding performance in concrete with electric arc furnace oxidizing slag aggregate. *J. Ceram. Process. Res.* **20**(4), 363–371 (2019)
- Lökçü, E.: Spinel mikrodalga dielektrik seramiklerinin polimerik jel yöntemi ile üretimi ve karakterizasyonu 1–72 (2013)
- Naseri, M.G., Saion, E.B., Ahangar, H.A., Hashim, M., Shaari, A.H.: Simple preparation and characterization of nickel ferrite nanocrystals by a thermal treatment method. *Powder Technol.* **212**(1), 80–88 (2011). <https://doi.org/10.1016/j.powtec.2011.04.033>
- Park, O.S., Cho, H.K.: EMP shielding of mortar mixed with SiC and graphite. *J. Ceram. Process. Res.* **23**(2), 165–170 (2022). <https://doi.org/10.36410/jcpr.2022.23.2.165>
- Peymanfar, R., Ghorbanian-Gezaforodi, S., Selseleh-Zakerin, E., Ahmadi, A., Ghaffari, A.: Tailoring  $\text{La}_{0.8}\text{Sr}_{0.2}\text{MnO}_3/\text{La}/\text{Sr}$  nanocomposite using a novel complementary method as well as dissecting its microwave, shielding, optical, and magnetic characteristics. *Ceram. Int.* **46**(13), 20896–20904 (2020a). <https://doi.org/10.1016/j.ceramint.2020.05.139>
- Peymanfar, R., Ahmadi, A., Selseleh-Zakerin, E.: Evaluation of the size and medium effects on the microwave absorbing, magnetic, electromagnetic shielding, and optical properties using  $\text{CuCo}_2\text{S}_4$  nanoparticles. *J. Alloys Compd.* **848**, 156453–156465 (2020b). <https://doi.org/10.1016/j.jallcom.2020.156453>
- Peymanfar, R., Yektaei, M., Javanshir, S., Selseleh-Zakerin, E.: Regulating the energy band-gap, UV–Vis light absorption, electrical conductivity, microwave absorption, and electromagnetic shielding effectiveness by modulating doping agent. *Polymer* **209**, 122981–122989 (2020c). <https://doi.org/10.1016/j.polymer.2020.122981>
- Peymanfar, R., Keykavous-Amand, S., Abadi, M.M., Yassi, Y.: A novel approach toward reducing energy consumption and promoting electromagnetic interference shielding efficiency in the buildings using brick/polyaniline nanocomposite. *Constr. Build. Mater.* **263**, 120042–120051 (2020d). <https://doi.org/10.1016/j.conbuildmat.2020.120042>
- Peymanfar, R., Selseleh-Zakerin, E., Ahmadi, A., Tavassoli, S.H.: Architecting functionalized carbon microtube/carrollite nanocomposite demonstrating significant microwave characteristics. *Sci. Rep.* **11**(1), 1–15 (2021a). <https://doi.org/10.1038/s41598-021-91370-5>
- Peymanfar, R., Selseleh-Zakerin, E., Ahmadi, A., Saeidi, A., Tavassoli, S.H.: Preparation of self-healing hydrogel toward improving electromagnetic interference shielding and energy efficiency. *Sci. Rep.* **11**(1), 1–12 (2021b). <https://doi.org/10.1038/s41598-021-95683-3>
- Peymanfar, R., Javanshir, S., Naimi-Jamal, M.R., Tavassoli, S.H.: Morphology and medium influence on microwave characteristics of nanostructures: a review. *J. Mater. Sci.* **56**(31), 17457–17477 (2021c). <https://doi.org/10.1007/s10853-021-06394-z>
- Peymanfar, R., Ahmadi, A., Selseleh-Zakerin, E., Ghaffari, A., Mojtahedi, M.M., Sharifi, A.: Electromagnetic and optical characteristics of wrinkled Ni nanostructure coated on carbon microspheres. *Chem. Eng. J.* **405**, 126985–126997 (2021e). <https://doi.org/10.1016/j.cej.2020.126985>
- Pratap, V., Soni, A.K., Dayal, S., Abbas, S.M., Siddiqui, A.M., Prasad, N.E.: Electromagnetic and absorption properties of U-type barium hexaferrite-epoxy composites. *J. Magn. Magn. Mater.* **465**, 540–545 (2018). <https://doi.org/10.1016/j.jmmm.2018.06.027>
- Pratap, V., Soni, A.K., Siddiqui, A.M., Abbas, S.M., Katiyar, R., Prasad, N.E.: Dielectric and radar-absorbing properties of exfoliated graphite dispersed epoxy composites. *J. Electron. Mater.* **49**(6), 3972–3981 (2020). <https://doi.org/10.1007/s11664-020-08118-6>
- Pratap, V., Soni, A.K., Abbas, S.M., Siddiqui, A.M., Prasad, N.E.: Effect of zinc substitution on U-type barium hexaferrite-epoxy composites as designed for microwave absorbing applications. *J. Alloys Compd.* **158280**–158290 (2021). <https://doi.org/10.1016/j.jallcom.2020.158280>
- Ren, F., Shi, Y., Ren, P., Si, X., Wang, H.: Cyanate ester resin filled with graphene nanosheets and  $\text{NiFe}_2\text{O}_4$ -reduced graphene oxide nanohybrids for efficient electromagnetic interference shielding. *NANO* **12**(6), 1–10 (2017). <https://doi.org/10.1142/S1793292017500667>
- Rohini, R., Bose, S.: Electromagnetic interference shielding materials derived from gelation of multiwall carbon nanotubes in polystyrene/poly(methyl methacrylate) blends. *ACS. Appl. Mater. Interfaces* **6**(14), 11302–11310 (2014)
- Şahin, E. İ.: Katkılı  $\text{NiFe}_2\text{O}_4$  polimer tabanlı mikrodalga yutucuların frekans seçici malzeme tasarımı 1–92 (2019)
- Şahin, E.İ.: Microwave electromagnetic shielding effectiveness of  $\text{znb}_2\text{o}_6$ -chopped strands composites for radar and wideband (6.5–18 GHz) applications. *Lith. J. Phys.* **62**(3), 161–170 (2022)
- Şahin, E.İ., Cantürk, S.B., Emek, M., Genç, S., Kartal, M.: Production and microwave electromagnetic shielding effectiveness of polyaniline- $\text{La}_2\text{Ti}_2\text{O}_7$ :Er yb composites. *J. Ceram. Process. Res.* **22**(2), 208–213 (2021). <https://doi.org/10.36410/jcpr.2021.22.2.208>

- Şahin, E.İ., Emek, M., Ertug, B., Kartal, M.: Radar ve daha geniş frekans aralığında kolemanit/PANI/SiO<sub>2</sub> Kompozitlerin elektromanyetik kalkanlama performansları. *Beykent Üniversitesi Fen ve Mühendislik Bilim Derg.* pp. 0–2. <https://doi.org/10.20854/bujse.742821> (2020)
- Thirumalairajan, S., Girija, K., Ganesh, V., Mangalaraj, D., Viswanathan, C., Ponpandian, N.: Novel synthesis of LaFeO<sub>3</sub> nanostructure dendrites: a systematic investigation of growth mechanism, properties, and biosensing for highly selective determination of neurotransmitter compounds. *Cryst. Growth Des.* **13**(1), 291–302 (2013). <https://doi.org/10.1021/cg3014305>
- Tihtih, M., Ibrahim, J.E.F.M., Kurovics, E., Gömze, L.A.: Study of the structure, microstructure and temperature dependent thermal conductivity properties of SrTiO<sub>3</sub>: via Y<sup>3+</sup> substitution. *J. Nano Res.* **69**, 33–42 (2021). <https://doi.org/10.4028/www.scientific.net/JNanoR.69.33>
- Tihtih, M., Eldin, J., Mohamed, F.M.I.: Enhanced optical and thermal conductivity properties of barium titanate ceramic via strontium doping for thermo—optical applications. *Opt. Quantum Electron.* **55**(3), 1–20 (2023). <https://doi.org/10.1007/s11082-022-04516-8>
- ur Rehman, S., Liu, J., Ahmed, R., Bi, H.: Synthesis of composite of ZnO spheres with polyaniline and their microwave absorption properties. *J. Saudi Chem. Soc.* **23**(4), 385–391 (2019). <https://doi.org/10.1016/j.jscs.2018.04.006>
- Yang, C.C., Gung, Y.J., Hung, W.C., Ting, T.H., Wu, K.H.: Infrared and microwave absorbing properties of BaTiO<sub>3</sub>/polyaniline and BaFe<sub>12</sub>O<sub>19</sub>/polyaniline composites. *Compos. Sci. Technol.* **70**(3), 466–471 (2010). <https://doi.org/10.1016/j.compscitech.2009.11.021>
- Yuping, D., Shunhua, L., Hongtao, G.: Investigation of electrical conductivity and electromagnetic shielding effectiveness of polyaniline composite. *Sci. Technol. Adv. Mater.* **6**(5), 513–518 (2005). <https://doi.org/10.1016/j.stam.2005.01.002>
- Zhao, X., Zhang, Y.L., Wang, X.X., Shi, H.L., Wang, W.Z., Cao, M.S.: Enhanced microwave absorption properties of NiFe<sub>2</sub>O nanocrystal deposited reduced graphene oxides. *J. Mater. Sci. Mater. Electron.* **27**(11), 11518–11523 (2016a). <https://doi.org/10.1007/s10854-016-5280-0>
- Zhao, C., Huang, W., Liu, X., Or, S.W., Cui, C.: Microwave absorbing properties of NiFe<sub>2</sub>O<sub>4</sub> nanosheets synthesized via a simple surfactant-assisted solution route. *Mater. Res.* **19**(5), 1149–1154 (2016b). <https://doi.org/10.1590/1980-5373-MR-2015-0581>

**Publisher's Note** Springer Nature remains neutral with regard to jurisdictional claims in published maps and institutional affiliations.

## Authors and Affiliations

Ethem İlhan Şahin<sup>1</sup> · Mehriban Emek<sup>2</sup> · Jamal Eldin F. M. Ibrahim<sup>3,4</sup> · Görkem Yumuşak<sup>5</sup> · Mesut Kartal<sup>6</sup>

<sup>1</sup> Advanced Technology Research and Application Center, Adana Alparslan Türkeş Science and Technology University, 01250 Adana, Turkey

<sup>2</sup> Department of Physics, Computer Technologies, Golbasi Vocational School, Adiyaman University, 02040 Gölbaşı, Adiyaman, Turkey

<sup>3</sup> Present Address: Department of Materials Technology, University of Bahri, Khartoum, Sudan

<sup>4</sup> Institute of Ceramic and Polymer Engineering, University of Miskolc, Egyetemvaros, Miskolc H-3515, Hungary

<sup>5</sup> Department of Metallurgical and Materials Engineering, Marmara University, 34722 Göztepe, Istanbul, Turkey

<sup>6</sup> Department of Electronics and Communication Engineering, İstanbul Technical University, 34469 Maslak, Istanbul, Turkey